AIMS Mathematics, 8(7): 16773–16789.
DOI: 10.3934/math.2023858
Received: 19 February 2023
Revised: 13 April 2023
Accepted: 23 April 2023
Published: 12 May 2023

http://www.aimspress.com/journal/Math

Research article

Impact of couple stress and variable viscosity on heat transfer and flow between two parallel plates in conducting field

Geetika Saini[1,†], B. N. Hanumagowda[1], S. V. K. Varma[1], Jasgurpreet Singh Chohan[2], Nehad Ali Shah[3,†] and Yongseok Jeon[4,*]

[1] Department of Mathematics, School of Applied Sciences, REVA University, Bengaluru, Karnataka, India
[2] Department of Mechanical Engineering and University Centre for Research & Development, Chandigarh University, Mohali-140413, Punjab
[3] Department of Mechanical Engineering, Sejong University, Seoul 05006, Korea
[4] Interdisciplinary Major of Maritime AI Convergence, Department of Mechanical Engineering, Korea Maritime & Ocean University, Busan 49112, Korea

* **Correspondence:** Email: ysjeon@kmou.ac.kr.

† These authors contributed equally to this work and are co-first authors.

Abstract: This study explores the flow properties of a couple stress fluid with the consideration of variable viscosity and a uniform transverse magnetic field. Under the effect of irreversible heat transfer, a steady fluid flow has taken place between two parallel inclined plates. The fluid flows due to gravity and the constant pressure gradient force. The plates are fixed and isothermal. The governing equations have been solved analytically for velocity and temperature fields. The total rate of heat flow and volume flow across the channel, skin friction, and Nusselt number at both plates are calculated and represent the impacts of relevant parameters through tables and graphs. The findings show that velocity, temperature, and the total rate of heat flow across the channel are enhanced by increasing the couple stress parameter and the viscosity variation parameter, while increasing the values of the Hartmann number reduces them.

Keywords: magnetic field; couple stress fluid; viscous dissipation; heat transfer; Lorentz force; variable viscosity
Mathematics Subject Classification: 35Q79, 93C20

1. Introduction

In recent years, the major problem encountered by many researchers has been in the sector of magnetohydrodynamic (MHD) flows and heat transfer because of their significant applications in MHD pumps, MHD generators, aerodynamic heating, the petroleum industry, plasma studies, etc. [1–3]. The heat transfer in non-Newtonian fluids is necessary for the dismemberment of molten plastics, substantial oils and greases, synthetic fibers, and foodstuffs because non-Newtonian fluids have multiple applications in many areas of industry, biology, and engineering [4,5]. Stokes [6,7] proposed a couple stress fluid as one non-Newtonian fluid.

Falade et al. [8] and Farooq et al. [9] examined the heat transfer problem of couple stress fluid flow with variable viscosity between parallel plates. Srinivasacharya et al. [10] analyzed the Hall and Ion-slip effects with a variable heat source and MHD on couple stress fluid flow between two circular cylinders using the homotopy analysis method (HAM) and illustrated the impact of different appearing parameters on velocity and temperature fields. Numerous research studies [11–16] have expanded on the existing problems of couple stress fluid flow by including MHD with various effects and geometries. The impact of heat transfer and MHD on third-grade fluid flow between two parallel plates has been numerically investigated by [17–19] and examined in terms of the characteristics of velocity and temperature fields. Makinde et al. [20] showed how MHD and radiative heat transport work together to affect an optically thin fluid with a porous medium. Ahmed [21] looked into the steady MHD flow of an electrically conducting viscous fluid with heat and mass transfer in a porous medium and thermal diffusion. Umavathi et al. [22] examined the MHD Poiseuille-Couette flow of two non-mixable fluids, one of which conducts electricity and the other of which doesn't. They also looked at how new factors affect the speed and temperature distributions. Ahmed et al. [23] analysed the MHD flow of an electrically conducting viscous fluid with heat transfer across infinite annular vertical cylinders subjected to a time-dependent pressure gradient and thermal radiation. Ogunmola et al. [24] and Shah et al. [25] investigated the nature of velocity and temperature distributions by changing relevant factors and taking into account third-grade fluid flow and variable viscosity. Hassan et al. [26] studied the influence of varying viscosity and MHD on a heat-producing porous couple stress fluid with a convective cooling wall. Makinde et al. [27] investigated the MHD heat and mass transport effects on nanofluids using Poiseuille-Couette flow with the consideration of Hall effects and varying viscosity. Umavathi et al. [28] presented the variation in velocity and temperature domains by changing the physical characteristics of a couple stress fluid sandwiched between two viscous fluid layers. Imran et al. [29] investigated the applications of non-integer Caputo time fractional derivatives to natural convection flow subject to arbitrary velocity and Newtonian heating. Shah et. al. [30] presented the General solution for MHD-free convection flow over a vertical plate with ramped wall temperature and chemical reaction.

The innovative characteristics and aims of this work are noted by the fact that transportation heat couple stress model involves MHD, viscous dissipation, temperature-dependent viscosity, and inclination of the channel. This mathematical model is appropriate for the advantages of biological and

lubrication systems. The behaviour of the fluid velocity, energy, skin friction and Nusselt number at the surfaces, total volume flow rate, and heat flow rate across the channel for various influential factors in the presence and absence of couple stress is discussed using graphs and tables.

2. Basic equations and description of the flow model

2.1. Basic equations

To discard the induced magnetic field, assuming the magnetic Reynolds number is very small. The current density is given by

$$\vec{J} = \sigma(\vec{q} \times \vec{B}), \tag{1}$$

The Lorentz force is defined as

$$\vec{J} \times \vec{B} = -\sigma {B_0}^2 \vec{q}, \tag{2}$$

The dimensional version of the continuity, momentum, and energy equations is as follows:

$$\vec{\nabla} \cdot \vec{q} = 0, \tag{3}$$

$$\rho\left[\frac{\partial \vec{q}}{\partial t} + (\vec{q} \cdot \vec{\nabla})\vec{q}\right] = -\vec{\nabla}p + \mu\nabla^2\vec{q} - \eta\nabla^4\vec{q} + \vec{J} \times \vec{B} + \rho\vec{g}, \tag{4}$$

$$\rho C_p\left[\frac{\partial \Theta}{\partial t} + (\vec{q} \cdot \vec{\nabla})\Theta\right] = \kappa\nabla^2\Theta + \varphi. \tag{5}$$

where $\vec{q}$ is the vector velocity, φ is the viscous dissipation of energy, C_p is the specific heat, $\vec{J}$ is the current density and B_0 is the applied magnetic field.

2.2. Description of the flow model

It is considered the steady flow of a couple stress fluid passing through two infinitely long parallel plates separated by $2h$, which are inclined from the surface at an angle of α. Plates are stable, and fluid flow is hydrodynamically and thermodynamically fully developed. The fluid is moving due to the axial pressure gradient and gravitational force. Θ_0 and Θ_1 are the temperatures at the bottom and top plates, respectively. A uniform magnetic field of intensity B_0 is applied, which is in a perpendicular direction to the fluid flow. The viscosity is temperature dependent. We have chosen a cartesian coordinate system such that the x-axis is along the central line of the channel and the y-axis is in a direction perpendicular to it, as seen in Figure 1.

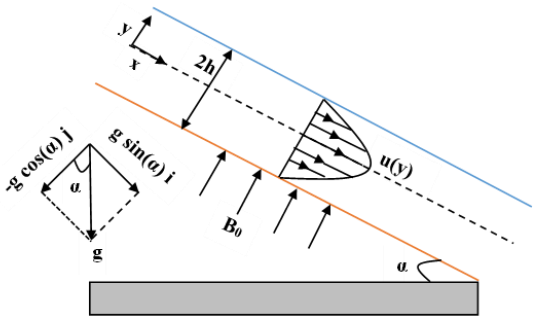

Figure 1. Flow model of the problem.

The channel is long enough so that all the physical quantities are functions of y alone, except the pressure. The velocity and temperature are as follows:

$$\vec{q} = (u(y), 0,0) and \Theta = \Theta(y). \tag{6}$$

Under the above assumptions, the Eqs (4) and (5) are transformed into

$$\eta \frac{d^4u}{dy^4} - \mu \frac{d^2u}{dy^2} - \left(\frac{d\mu}{dy}\right)\left(\frac{du}{dy}\right) + \frac{\partial p}{\partial x} - \rho g\, sin(\alpha) + \sigma {B_0}^2 u = 0, \tag{7}$$

$$\frac{d^2\Theta}{dy^2} + \frac{\mu}{\kappa}\left(\frac{du}{dy}\right)^2 + \frac{\eta}{\kappa}\left(\frac{d^2u}{dy^2}\right)^2 = 0, \tag{8}$$

The boundary conditions of the flow model are

$$\left.\begin{aligned} Aty = -h, u(y) = 0, u''(y) = 0, \Theta(y) = \Theta_0, \\ Aty = h, u(y) = 0, u''(y) = 0, \Theta(y) = \Theta_1. \end{aligned}\right\} \tag{9}$$

The temperature-dependent viscosity by Reynold's model [16,31–33] is given by

$$\mu(\Theta) = \mu_0 e^{-\beta(\Theta - \Theta_0)}. \tag{10}$$

Introducing the non-dimensional parameters [4,16] are as follows:

$$y^* = \frac{y}{h}, x^* = \frac{x}{h}, u^* = \frac{u}{U_0}, \Theta^* = \frac{\Theta - \Theta_0}{\Theta_1 - \Theta_0}, \mu^* = \frac{\mu}{\mu_0}, p^* = \frac{ph}{\mu_0 U_0}, m = \beta(\Theta_1 - \Theta_0),$$

$$Br = \frac{\mu_0 {U_0}^2}{\kappa(\Theta_1 - \Theta_0)}, B^2 = \frac{\mu_0 h^2}{\eta}, G = G_1 + G_2\, sin(\alpha), M^2 = \frac{\sigma {B_0}^2 h^2}{\mu_0}. \tag{11}$$

where $G_1 = -\frac{\partial p}{\partial x}$ is the pressure gradient parameter and $G_2 = \frac{h^2}{U_0 \mu_0}\rho g$ is the gravitational force parameter.

Equations (7) and (8) in the non-dimensional form (remove asterisks)

$$\frac{d^4u}{dy^4} - B^2\mu \frac{d^2u}{dy^2} - B^2 \frac{d\mu}{dy}\frac{du}{dy} - B^2 G + B^2 M^2 u = 0, \tag{12}$$

$$\frac{d^2\Theta}{dy^2} + Br\mu\left(\frac{du}{dy}\right)^2 + \frac{Br}{B^2}\left(\frac{d^2u}{dy^2}\right)^2 = 0, \tag{13}$$

and the boundary conditions (9) reduced into

$$\left.\begin{aligned} Aty = -1, u(y) = 0, u''(y) = 0, \Theta(y) = 0, \\ Aty = 1, u(y) = 0, u''(y) = 0, \Theta(y) = 1. \end{aligned}\right\} \tag{14}$$

The dimensionless form of Eq (10) is

$$\mu(\Theta) = e^{-m\Theta}. \tag{15}$$

Use the Taylor's series, Eq (15) reduced into

$$\mu(\Theta) = 1 - m\Theta, \frac{d\mu}{dy} = -m\frac{d\Theta}{dy}. \tag{16}$$

Substitute Eq (16) in Eqs (12) and (13), then the equations are transformed in the form:

$$\frac{d^4u}{dy^4} - B^2(1 - m\Theta)\frac{d^2u}{dy^2} + B^2 m\frac{d\Theta}{dy}\frac{du}{dy} - B^2G + B^2M^2u = 0, \tag{17}$$

$$\frac{d^2\Theta}{dy^2} + Br(1 - m\Theta)\left(\frac{du}{dy}\right)^2 + \frac{Br}{B^2}\left(\frac{d^2u}{dy^2}\right)^2 = 0. \tag{18}$$

2.3. Solution of the problem

Using the regular perturbation technique by taking the viscosity variation parameter m as a perturbation parameter where $0<m<<1$, to solve the above non-linear coupled equations, and the velocity and temperature expressions are given by:

$$u = u_0 + mu_1, \Theta = \Theta_0 + m\Theta_1. \tag{19}$$

Substitute Eq (19) in Eqs (14), (17) and (18) and separating each order of approximation provides:
Zeroth order equations:

$$\frac{d^4u_0}{dy^4} - B^2\frac{d^2u_0}{dy^2} - B^2G + B^2M^2u_0 = 0, \tag{20}$$

$$\frac{d^2\Theta_0}{dy^2} + Br\left(\frac{du_0}{dy}\right)^2 + \frac{Br}{B^2}\left(\frac{d^2u_0}{dy^2}\right)^2 = 0, \tag{21}$$

$$Aty = -1, u_0(y) = 0, u_0''(y) = 0, \Theta_0(y) = 0,$$

$$Aty = 1, u_0(y) = 0, u_0''(y) = 0, \Theta_0(y) = 1. \tag{22}$$

First order equations:

$$\frac{d^4u_1}{dy^4} - B^2\frac{d^2u_1}{dy^2} + B^2\Theta_0\frac{d^2u_0}{dy^2} + B^2\left(\frac{d\Theta_0}{dy}\right)\left(\frac{du_0}{dy}\right) + B^2M^2u_1 = 0, \tag{23}$$

$$\frac{d^2\Theta_1}{dy^2} + 2Br\left(\frac{du_0}{dy}\right)\left(\frac{du_1}{dy}\right) - Br\Theta_0\left(\frac{du_0}{dy}\right)^2 + \frac{2Br}{B^2}\left(\frac{d^2u_0}{dy^2}\right)\left(\frac{d^2u_1}{dy^2}\right) = 0, \tag{24}$$

$$Aty = -1, u_1(y) = 0, u_1''(y) = 0, \Theta_1(y) = 0,$$

$$Aty = 1, u_1(y) = 0, u_1''(y) = 0, \Theta_1(y) = 0. \tag{25}$$

Solve the zeroth and first order equations with their corresponding boundary conditions.

The solution for velocity and temperature distributions are obtained as:

$$\begin{aligned} u(y) = {} & \Omega_0 + \Omega_1\, cosh[Py] - \Omega_2\, cosh[Ry] + m\{\Omega_3\, cosh[Py] + \Omega_4\, sinh[Py] \\ & + \Omega_5\, cosh[Ry] + \Omega_6\, sinh[Ry] + \Omega_7\, cosh[3Py] + \Omega_8\, cosh[3Ry] \\ & + \Omega_9\, cosh[(P+2R)y] + \Omega_{10}\, cosh[(P-2R)y] + \Omega_{11}\, cosh[(2P+R)y] \\ & + \Omega_{12}\, cosh[(2P-R)y] + y(\Omega_{13}\, sinh[Py] + \Omega_{14}\, cosh[Py] \\ & + \Omega_{15}\, sinh[Ry] + \Omega_{16}\, cosh[Ry]) + y^2(\Omega_{17}\, sinh[Py] + \Omega_{18}\, cosh[Py] \\ & + \Omega_{19}\, sinh[Ry] + \Omega_{20}\, cosh[Ry]) + y^3(\Omega_{21}\, sinh[Py] + \Omega_{22}\, sinh[Ry])\}, \end{aligned} \tag{26}$$

$$\Theta(y) = \gamma_0 + \gamma_1 y + \gamma_2 y^2 + \gamma_3\, cosh[2Py] + \gamma_4\, cosh[2Ry] + \gamma_5\, cosh[(P+R)y]$$

$$+\gamma_6\cosh[(P-R)y]+m\{\gamma_7+\gamma_8\sinh[2Py]+\gamma_9\cosh[2Py]+\gamma_{10}\cosh[4Py]$$
$$+\gamma_{11}\sinh[2Ry]+\gamma_{12}\cosh[2Ry]+\gamma_{13}\cosh[4Ry]+\gamma_{14}\cosh[(P+R)y]$$
$$+\gamma_{15}\cosh[(P-R)y]+\gamma_{16}\sinh[(P+R)y]+\gamma_{17}\sinh[(P-R)y]$$
$$+\gamma_{18}\cosh[(P+3R)y]+\gamma_{19}\cosh[(P-3R)y]+\gamma_{20}\cosh[2(P+R)y]$$
$$+\gamma_{21}\cosh[2(P-R)y]+\gamma_{22}\cosh[(3P+R)y]+\gamma_{23}\cosh[(3P-R)y]$$
$$+y(\gamma_{24}+\gamma_{25}\sinh[2Py]+\gamma_{26}\cosh[2Py]+\gamma_{27}\cosh[(P+R)y]+\gamma_{28}\cosh[(P-R)y]$$
$$+\gamma_{29}\sinh[(P+R)y]+\gamma_{30}\sinh[(P-R)y]+\gamma_{31}\cosh[2Ry]+\gamma_{32}\sinh[2Ry])$$
$$+y^2(\gamma_{33}+\gamma_{34}\sinh[2Py]+\gamma_{35}\cosh[2Py]+\gamma_{36}\cosh[(P+R)y]+\gamma_{37}\cosh[(P-R)y]$$
$$+\gamma_{38}\sinh[(P+R)y]+\gamma_{39}\sinh[(P-R)y]+\gamma_{40}\sinh[2Ry]+\gamma_{41}\cosh[2Ry])+y^3(\gamma_{42}$$
$$+\gamma_{43}\sinh[2Py]+\gamma_{44}\sinh[2Ry]+\gamma_{45}\sinh[(P+R)y]+\gamma_{46}\sinh[(P-R)y])+\gamma_{47}y^4\}. \quad (27)$$

where Ω_i and γ_j, $i=1,2\ldots\ldots22$ and $j=1,2\ldots\ldots47$ are constants.

2.4. Volume flow rate, total heat flow rate, coefficient of Skin friction and Nusselt number

The volume flow rate across the channel

$$Q=\int_{-1}^{1}u(y)dy, \quad (28)$$

By Eq (26),

$$Q=2\{\Omega_0+\frac{1}{P^4}\left(P^3\Omega_1+m(P^3\Omega_3-P^2\Omega_{13}+P(2+P^2)\Omega_{18}-(6+3P^2)\Omega_{17})\right)\sinh[P]$$
$$+\frac{1}{R^4}\left(-R^3\Omega_2+m(R^3\Omega_5-R^2\Omega_{15}+R(2+R^2)\Omega_{20}-(6+3R^2)\Omega_{22})\right)\sinh[R]$$
$$+\frac{m}{P^3}(P^2\Omega_{13}-2P\Omega_{18}+(6+P^2)\Omega_{21})\cosh[P]+\frac{m}{R^3}(R^2\Omega_{15}-2R\Omega_{20}+(6+R^2)\Omega_{22})$$
$$\cosh[R]+\frac{m\Omega_7}{3P}\sinh[3P]+\frac{m\Omega_8}{3R}\sinh[3R]+\frac{m\Omega_9}{(P+2R)}\sinh[P+2R]$$
$$+\frac{m\Omega_{10}}{(P-2R)}\sinh[P-2R]+\frac{m\Omega_{11}}{(2P+R)}\sinh[2P+R]+\frac{m\Omega_{12}}{(2P-R)}\sinh[2P-R]\Big\}. \quad (29)$$

Total heat flow rate across the channel is given by

$$E=\int_{-1}^{1}u(y)\Theta(y)dy \quad (30)$$

At the lower plate, the skin friction coefficient C_f and Nusselt number Nu are given by

$$C_f=\mu\frac{du}{dy}\Big|_{y=-1},Nu=\frac{\partial\Theta}{\partial y}\Big|_{y=-1}, \quad (31)$$

At the upper plate, C_f and Nu are given by

$$C_f=-\mu\frac{du}{dy}\Big|_{y=1},Nu=-\frac{\partial\Theta}{\partial y}\Big|_{y=1}. \quad (32)$$

The negative sign is present because the top plate is positioned in the opposite direction of the fluid flow.

3. Results and discussion

This section includes the variation of velocity and temperature profiles and a discussion of

different values of the pressure gradient parameter G_1, viscosity variation parameter m, the Brinkman number Br, the Hartmann number M, the angle of inclination α, and the couple stress parameter B. We also discussed the variation of volume flux, skin friction coefficient C_f, and the Nusselt number Nu on both plates through surface graphs.

Figure 2 shows that with the increase of m, the fluid viscosity decreases, and the viscous heating enhances, due to which the velocity increases.

Figure 3 depicts that the higher the pressure gradient, the faster the stream flows, and hence velocity increases.

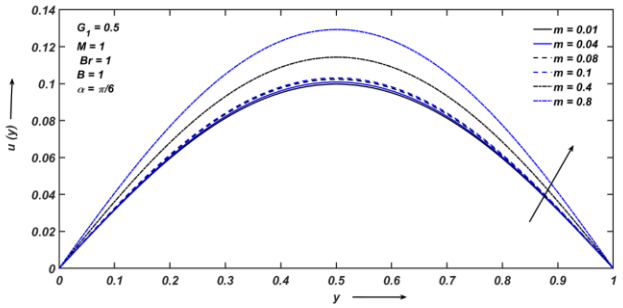

Figure 2. Velocity profile influenced by viscosity variation parameter.

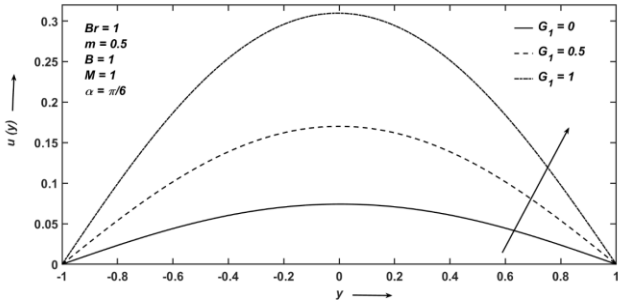

Figure 3. Velocity profile affected by pressure gradient parameter.

According to Figure 4, a rise in B slows the motion of the fluid particles, providing them with enough force to pull off the frictional hindrance inboard the fluid and increase velocity in this manner.

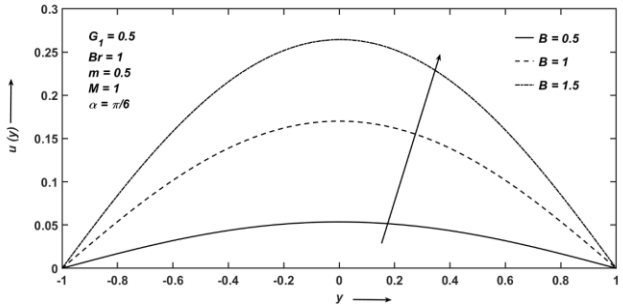

Figure 4. Velocity profile influenced by couple stress parameter.

Figure 5 shows that on increasing the values of *Br*, viscous dissipation dominates, due to which the velocity increases because the Brinkman number is the proportion of viscous heating to molecular conduction.

Figure 6 portrays that by raising the values of *M*, the Lorentz force gets stronger, which creates a resistive force in the fluid flow and causes the speed to slow down.

Figure 7 illustrates that as the angle of the inclined channel gets bigger, so does the velocity because fluid moves faster in a vertical channel than in a horizontal channel due to gravity.

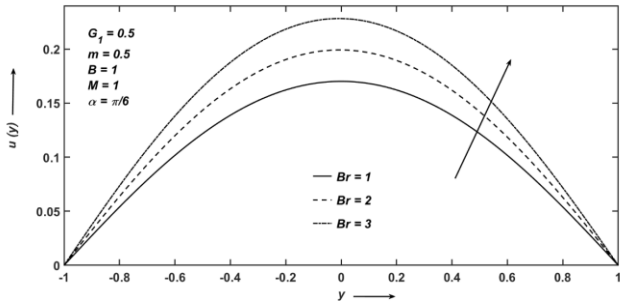

Figure 5. Velocity profile affected by Brinkman number.

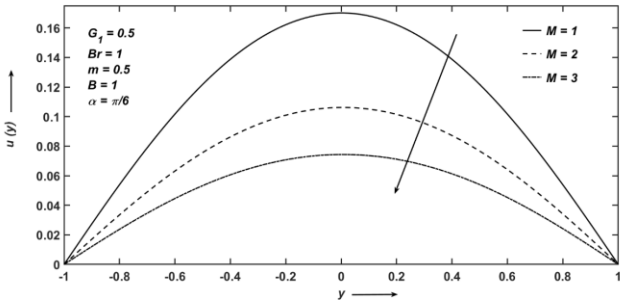

Figure 6. Velocity profile affected by the Hartmann number.

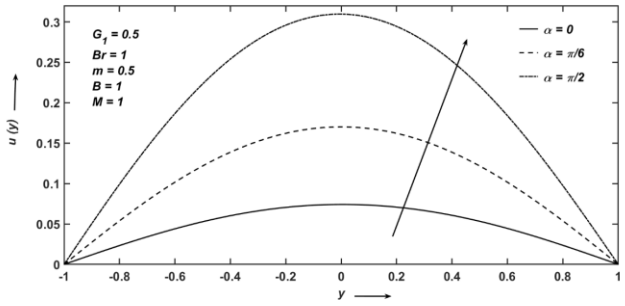

Figure 7. Velocity profile influenced by the angle of inclined channel.

According to Figures 8 and 9, raising the values of *m* and G_1 increases the viscous dissipation due to velocity and gradient, which enhances the fluid temperature.

Figure 10 shows that when *B* increases, so does the temperature in the flow channel due to the

viscous heating of the fluid particles.

Figure 11 displays that if *Br* increases, then heat production through viscous dissipation enhances, resulting in a temperature increase.

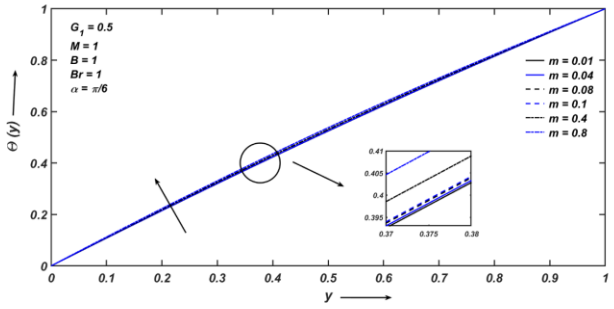

Figure 8. Temperature profile affected by viscosity variation parameter.

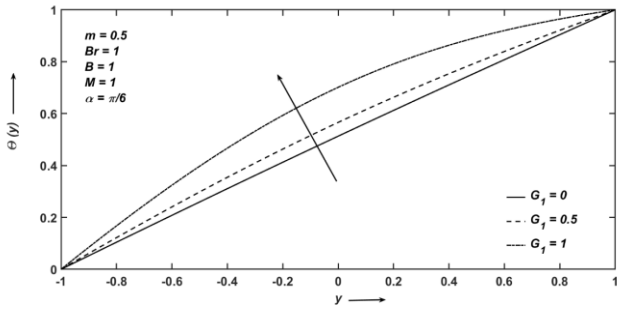

Figure 9. Temperature profile affected by pressure gradient parameter.

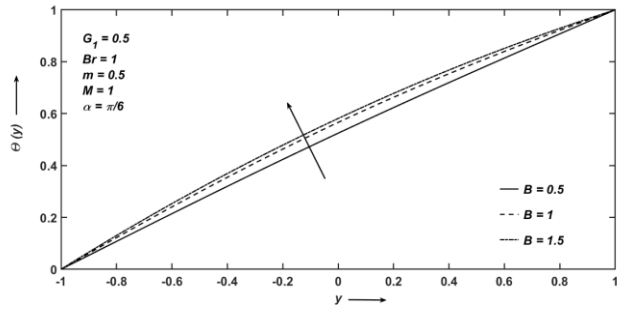

Figure 10. Temperature profile affected by couple stress parameter.

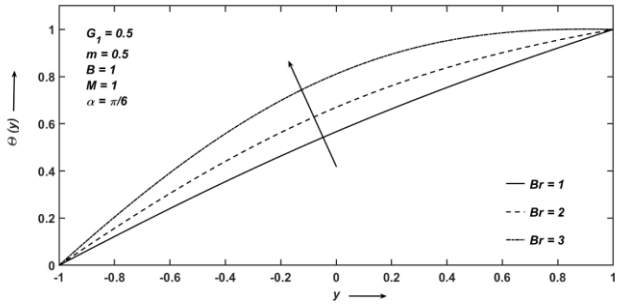

Figure 11. Temperature profile affected by Brinkman number.

Figure 12 exhibits the variation in M. An increase in Hartmann's number strengthens the Lorentz force, which acts against the fluid flow and so lowers the fluid temperature.

Figure 13 represents that as raising the value of α, causing the channel to become vertical, due to which the frictional force in fluid flow increases and so does the temperature.

Figure 14 shows that when the Brinkman number and viscosity parameter rise, so does heat production from viscous dissipation. This makes the volume flow rate across the channel go up.

Figure 15(a) portrays the coefficient of skin friction C_f at the lower plate. It shows that when both Br and m grow at the same time, and when one of the parameters rises while the other remains unchanged, then the C_f increases. Figure 15(b) illustrates C_f at the upper plate. It shows that C_f grows with the increase of Br, whereas C_f initially increases for $0 \leq m \leq 0.3$ and starts to decrease gradually for further increases in m.

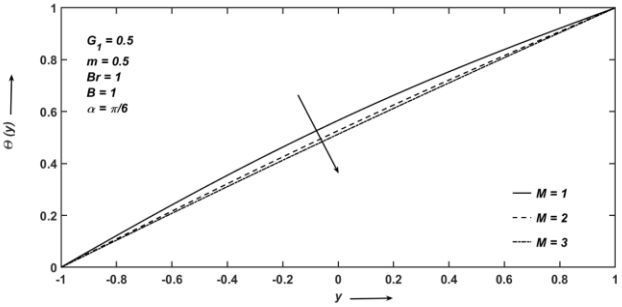

Figure 12. Temperature profile affected by Hartmann number.

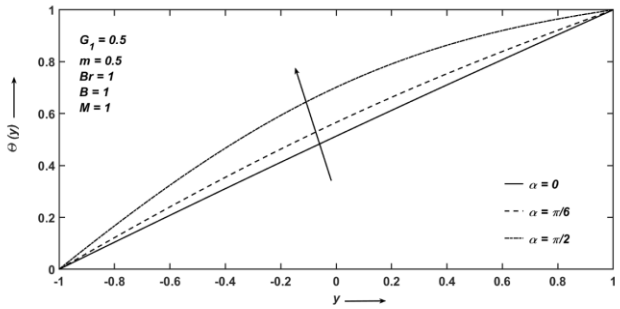

Figure 13. Temperature profile affected by angle of inclined channel.

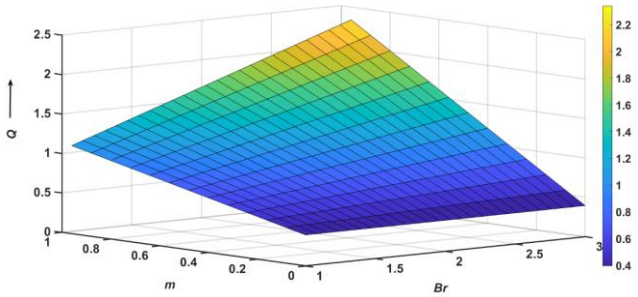

Figure 14. Surface graph for Volume flux.

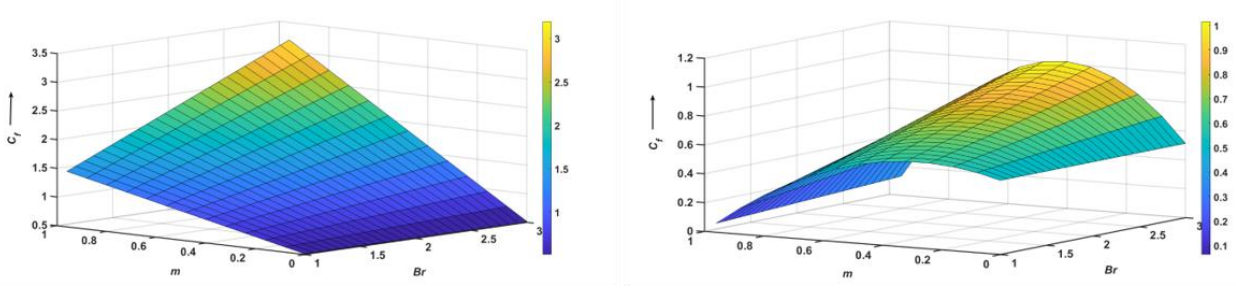

Figure 15. Variation for the coefficient of skin friction at the (a) lower plate and (b) upper plate.

Figure 16(a) and Figure 16(b) depict that when both Br and m increase in parallel time and if one of the parameters grows while the other stays constant, then the heat transfer irreversibility due to convection is more dominant and the temperature gradient rises, and hence the Nusselt number Nu at both the plates increases.

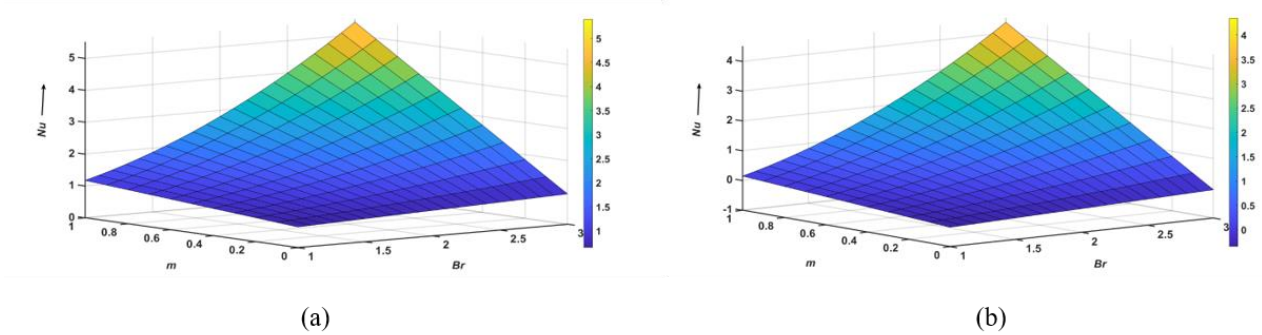

Figure 16. Variation for Nusselt number at the (a) lower plate and (b) upper plate.

Table 1. Results for total heat flow rate by considering $G_1 = 0.5, Br = 1$ and $\alpha = \frac{\pi}{6}$.

M	*B*	*M*	*E*
0	1	1	0.0908
0.4	1	1	0.1145
0.8	1	1	0.1393
0.5	0.5	1	0.0356
0.5	1	1	0.1206
0.5	1.5	1	0.1929
0.5	1	1	0.1206
0.5	1	2	0.0713
0.5	1	3	0.0491

Table 1 represents the findings for the total rate of heat flow by varying the viscosity parameter, couple stress parameter, and the Hartmann number. The total heat flow rate increases as *m* and *B* increase, but higher Hartmann numbers lower the heat flow rate.

4. Validation

4.1. M=α=0

The current investigation in the absence of a magnetic field with the horizontal channel ($\alpha=0$) and the transformation $y' = \frac{y+h}{2}$ validates the previously investigated work by Falade et al. [8].

The results are identical, which are represented in Figures 17 and 18 and Table 2 for the velocity profile by varying the Brinkman number, viscosity parameter, and couple stress parameter.

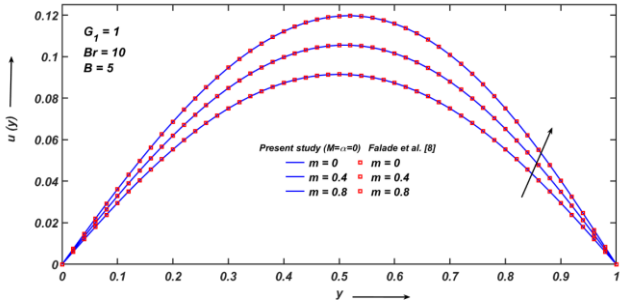

Figure 17. Comparison for velocity profile by varying viscosity variation parameter.

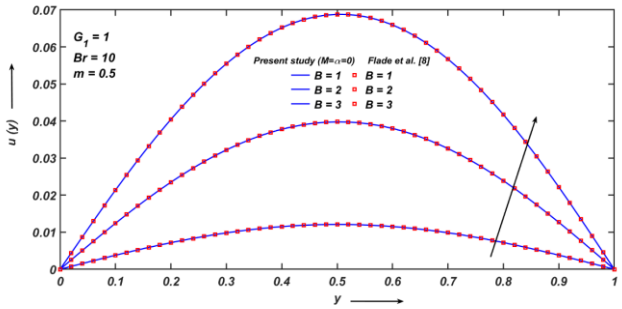

Figure 18. Comparison for velocity profile by varying couple stress parameter.

Table 2. Comparison of *u(y)* by considering $G_1=1$, $m=0.5$ *and* $B=10$.

Br	Falade et al. [8]	Present study *(M=α=0)*
1	0.1417	0.1417
50	0.1508	0.1508
100	0.1601	0.1601

4.2. M=B=α=0

The current study in the absence of a magnetic field and couple stress with the horizontal channel ($\alpha=0$) and the transformation $y' = \frac{y+h}{2}$ validates the previously investigated work by O D Makinde [32].

For the velocity profile with variable viscosity parameter and Brinkman number, the findings shown in Figures 19 and 20 are equal.

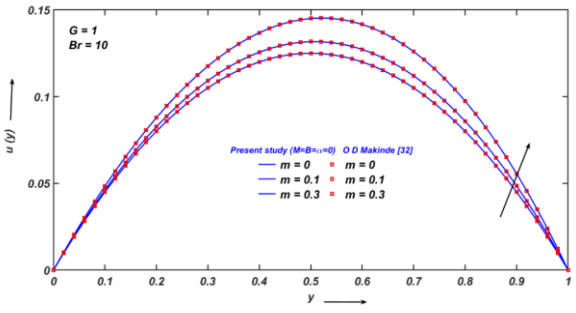

Figure 19. Comparison for velocity profile by varying viscosity variation parameter.

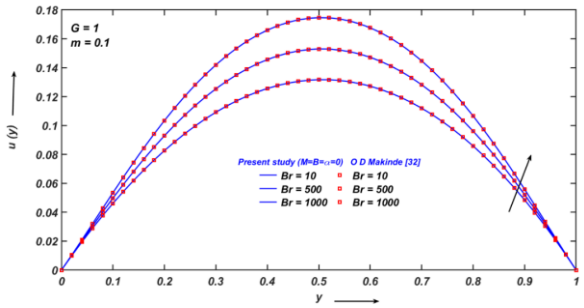

Figure 20. Comparison for velocity profile by varying Brinkman number.

5. Conclusions

The impact of MHD and temperature-dependent viscosity on couple stress fluid flow has been studied between two heated inclined parallel plates. The effects of relevant parameters on the fields of velocity, temperature, volume flow rate, total heat flow rate, coefficient of skin friction, and Nusselt number are concluded as follows:

- Velocity and temperature enhance with an increase in the pressure gradient, viscosity variation, couple stress parameters, Brinkman number, and angle of the inclined channel, whereas both reduce as the Hartmann number grows.
- The rate of volume flow across the channel increases as the viscosity variation parameter and Brinkman number increase.
- As the viscosity variation and couple stress parameters rise, the total rate of heat flow across the channel enhances, but it declines as the Hartmann number goes up.
- At the lower plate, skin friction increases as the viscosity variation parameter and Brinkman number increase. At the upper plate, it grows as the Brinkman number increases, whereas with the variation of the viscosity parameter, it initially increases and then gradually declines.
- The Nusselt number at both plates increases as the viscosity variation parameter and Brinkman number increase.

Acknowledgments

Geetika would like to express her heartfelt gratitude to CSIR-UGC for their financial support with grant no. 09/1313(0001)/2020-EMR-I. This study was supported by the National Research Foundation of Korea (NRF) funded by the Korean government (MSIT) [NRF-2021R1I1A3047845, NRF-2022R1A4A3023960] and BK21 Four program through the National Research Foundation of Korea (NRF) funded by the Ministry of Education of Korea (Center for Creative Leaders in Maritime Convergence).

Conflict of interest

The authors declare no conflict of interest.

References

1. A. Bég, A. Y. Bakier, V. R. Prasad, J. Zueco, S. K. Ghosh, Nonsimilar, laminar, steady, electrically-conducting forced convection liquid metal boundary layer flow with induced magnetic field effects, *Int. J. Therm. Sci.*, **48** (2009), 1596–1606. https://doi.org/10.1016/j.ijthermalsci.2008.12.007
2. A. Setayesh, V. Sahai, Heat transfer in developing magnetohydrodynamic Poiseuille flow and variable transport properties, *Int. J. Heat Mass Tran.*, **33** (1990), 1711–1720. https://doi.org/10.1016/0017-9310(90)90026-Q
3. N. A. Shah, A. Ebaid, T. Oreyeni, S. J. Yook, MHD and porous effects on free convection flow of viscous fluid between vertical parallel plates: advance thermal analysis, *Waves in Random and Complex Media*, 2023. https://doi.org/10.1080/17455030.2023.2186717
4. M. Farooq, M. T. Rahim, S. Islam, A. M. Siddiqui, Steady Poiseuille flow and heat transfer of couple stress fluids between two parallel inclined plates with variable viscosity, *J. Assoc. Arab Univ. Basic Appl. Sci.*, **14** (2013), 9–18. https://doi.org/10.1016/j.jaubas.2013.01.004
5. A. Khan, M. Farooq, R. Nawaz, M. Ayza, H. Ahmad, H. Abu-Zinadah, et al., Analysis of couple stress fluid flow with variable viscosity using two homotopy-based methods, *Open Phys.*, **19** (2021), 134–145. https://doi.org/10.1515/phys-2021-0015
6. V. K. Stokes, Couple stresses in fluids, *Phys. Fluids*, **9** (1996), 1709–1715. https://doi.org/10.1063/1.1761925
7. V. K. Stokes, Couple stresses in fluids, In: *Theories of fluids with microstructure*, Heidelberg: Springer, 1984. https://doi.org/10.1007/978-3-642-82351-0_4
8. J. A. Falade, S. O. Adesanya, J. C. Ukaegbu, M. O. Osinowo, Entropy generation analysis for variable viscous couple stress fluid flow through a channel with non-uniform wall temperature, *Alex. Eng. J.*, **55** (2016), 69–75. https://doi.org/10.1016/j.aej.2016.01.011
9. M. Farooq, S. Islam, M. T. Rahim, T. Haroon, Heat transfer flow of steady couple stress fluids between two parallel plates with variable viscosity, *Heat Transf. Res.*, **42** (2011), 737–780. https://doi.org/10.1615/HeatTransRes.2012000996
10. D. Srinivasacharya, K. Kaladhar, Analytical solution of MHD free convective flow of couple stress fluid in an annulus with Hall and ion-slip effects, *Nonlinear Anal. Model. Control*, **16** (2011), 477–487. https://doi.org/10.15388/NA.16.4.14090
11. S. Jangili, S. O. Adesanya, H. A. Ogunseye, R. Lebelo, Couple stress fluid flow with variable properties: A second law analysis, *Math. Method. Appl. Sci.*, **42** (2019), 85–98. https://doi.org/10.1002/mma.5325
12. N. T. M. EL-Dabe, S. M. G. EL-Mohandis, Effect of couple stresses on pulsatile hydromagnetic poiseuille flow, *Fluid Dyn. Res.*, **15** (1995), 313–324. https://doi.org/10.1016/0169-5983(94)00049-6
13. L. Jayaraman, G. Ramanaiah, Effect of couple stresses on transient MHD poiseuille flow, *J. Comput. Phys.*, **60** (1985), 478–488. https://doi.org/10.1016/0021-9991(85)90032-4
14. K. Ramesh, Influence of heat and mass transfer on peristaltic flow of a couple stress fluid through porous medium in the presence of inclined magnetic field in an inclined asymmetric channel, *J. Mol. Liq.*, **219** (2016), 256–271. https://doi.org/10.1016/j.molliq.2016.03.010

15. M. Dhlamini, H. Mondal, P. Sibanda, S. Motsa, Numerical analysis of couple stress nanofluid in temperature dependent viscosity and thermal conductivity, *Int. J. Appl. Comput. Math.*, **7** (2021), 48. https://doi.org/10.1007/s40819-021-00983-x
16. R. Ellahi, A. Zeeshan, F. Hussain, T. Abbas, Two-phase Couette flow of couple stress fluid with temperature dependent viscosity thermally affected by magnetized moving surface, *Symmetry*, **11** (2019), 647. https://doi.org/10.3390/sym11050647
17. L. Wang, Y. Jian, Q. Liu, F. Li, L. Chang, Electromagnetohydrodynamic flow and heat transfer of third grade fluids between two micro-parallel plates, *Colloid. Surface. A*, **494** (2016), 87–94. https://doi.org/10.1016/j.colsurfa.2016.01.006
18. Y. M. Aiyesimi, G. T. Okedayo, O. W. Lawal, Unsteady magnetohydrodynamic (MHD) thin film flow of a third grade fluid with heat transfer and no slip boundary condition down an inclined plane, *Int. J. Phys. Sci.*, **8** (2013), 946–955. https://doi.org/10.5897/IJPS2013.3891
19. Z. Shao, N. A. Shah, I. Tlili, U. Afzal, S. Khan, Hydromagnetic free convection flow of viscous fluid between vertical parallel plates with damped thermal and mass fluxes, *Alex. Eng. J.*, **58** (2019), 989–1000. https://doi.org/10.1016/j.aej.2019.09.001
20. O. Makinde, P. Y. Mhone, Heat transfer to MHD oscillatory flow in a channel Ölled with porous medium, *Rom. J. Phys.*, **50** (2005), 931–938.
21. N. Ahmed, Heat and mass transfer in MHD Poiseuille flow with porous walls, *J. Eng. Phys. Thermophys.*, **92** (2019), 122–131. https://doi.org/10.1007/s10891-019-01914-w
22. J. Umavathi, I. C. Liu, P. Kumar, Magnetohydrodynamic Poiseuille-Couette flow and heat transfer in an inclined channel, *J. Mech.*, **26** (2010), 525–532. https://doi.org/10.1017/S172771910000472X
23. N. Ahmed, M. Dutta, Heat transfer in an unsteady MHD flow through an infinite annulus with radiation, *Bound. Value Probl.*, **2015** (2015), 11. https://doi.org/10.1186/s13661-014-0279-z
24. B. Ogunmola, A. Akinshilo, G. Sobamowo, Perturbation solutions for Hagen-Poiseuille flow and heat transfer of third-grade fluid with temperature-dependent viscosities and internal heat generation, *Int. J. Eng. Math.*, **2016** (2016), 8915745. https://doi.org/10.1155/2016/8915745
25. R. A. Shah, S. Islam, A. M. Siddiqui, T. Haroon, Heat transfer by laminar flow of a third grade fluid in wire coating analysis with temperature dependent and independent viscosity, *Anal. Math. Phys.*, **1** (2011), 147–166. https://doi.org/10.1007/s13324-011-0011-4
26. A. R. Hassan, S. O. Salawu, A. B. Disu, The variable viscosity effects on hydromagnetic couple stress heat generating porous fluid flow with convective wall cooling, *Sci. Afr.*, **9** (2020), e00495. https://doi.org/10.1016/j.sciaf.2020.e00495
27. O. D. Makinde, T. Iskander, F. Mabood, W. A. Khan, M. S. Tshehla, MHD Couette-Poiseuille flow of variable viscosity nanofluids in a rotating permeable channel with Hall effects, *J. Mol. Liq.*, **221** (2016), 778–787. https://doi.org/10.1016/j.molliq.2016.06.037
28. J. C. Umavathi, A. J. Chamkha, M. H. Manjula, A. Al-Mudhaf, Flow and heat transfer of a couple-stress fluid sandwiched between viscous fluid layers, *Can. J. Phys.*, **83** (2005), 705–720. https://doi.org/10.1139/p05-032
29. M. A. Imran, N. A. Shah, I. Khan, M. Aleem, Applications of non-integer Caputo time fractional derivatives to natural convection flow subject to arbitrary velocity and Newtonian heating, *Neural Comput. Appl.,* **30** (2018**)**, 1589–1599. https://doi.org/10.1007/s00521-016-2741-6

30. N. A. Shah, A. A. Zafar, S. Akhtar, General solution for MHD-free convection flow over a vertical plate with ramped wall temperature and chemical reaction, *Arab. J. Math.,* **7** (2018), 49–60. https://doi.org/10.1007/s40065-017-0187-z
31. O. D. Makinde, Laminar falling liquid film with variable viscosity along an inclined heated plate, *Appl. Math. Comput.*, **175** (2006), 80–88. https://doi.org/10.1016/j.amc.2005.07.021
32. O. D. Makinde, Entropy-generation analysis for variable-viscosity channel flow with non-uniform wall temperature, *Appl. Energy*, **85** (2008), 384–393. https://doi.org/10.1016/j.apenergy.2007.07.008
33. A. B. Disu, M. S. Dada, Reynold's model viscosity on radiative MHD flow in a porous medium between two vertical wavy walls, *J. Taibah Univ. Sci.*, **11** (2017), 548–565. https://doi.org/10.1016/j.jtusci.2015.12.001

AIMS Press